Geophys. J. Int. (2009) **176,** 822–832 doi: 10.1111/j.1365-246X.2008.04016.x

Temperature-dependent poroelastic and viscoelastic effects on microscale—modelling of seismic reflections in heavy oil reservoirs

Radim Ciz,[1] Erik H. Saenger,[2] Boris Gurevich[3] and Serge A. Shapiro[4]

[1]*Freie Universität Berlin, Fachrichtung Geophysik, Malteserstrasse* 74-100, *Build.* D, 12249 *Berlin, Germany. E-mail: ciz@geophysik.fu-berlin.de*
[2]*ETH Zurich, Geological Institute, Leonhardstrasse* 19, 8092 *Zurich, Switzerland and Spectraseis, Giessereistrasse* 5, 8005 *Zurich, Switzerland*
[3]*Department of Exploration Geophysics, Curtin University of Technology,* GPO Box U1987, *Perth, Western Australia* 6845 *and CSIRO Petroleum, ARRC,* 26 *Dick Perry Avenue, Kensington, Perth,* WA 6151, *Australia*
[4]*Freie Universität Berlin, Fachrichtung Geophysik, Malteserstrasse* 74-100, *Build.* D, 12249 *Berlin, Germany*

Accepted 2008 October 17. Received 2008 October 17; in original form 2007 July 12

SUMMARY

We develop a new model for elastic properties of rocks saturated with heavy oil. The heavy oil is represented by a viscoelastic material, which at low frequencies and/or high temperatures behaves as a Newtonian fluid, and at high frequencies and/or low temperatures as a nearly elastic solid. The bulk and shear moduli of a porous rock saturated with such viscoelastic material are then computed using approximate extended Gassmann equations of Ciz and Shapiro by replacing the elastic moduli of the pore filling material with complex and frequency-dependent moduli of the viscoelastic pore fill.

We test the proposed model by comparing its predictions with numerical simulations based on a direct finite-difference solution of equations of dynamic viscoelasticity. The simulations are performed for the reflection coefficient from an interface between a homogeneous fluid and a porous medium. The numerical tests are performed both for an idealized porous medium consisting of alternating solid and viscoelastic layers, and for a more realistic 3-D geometry of the pore space. Both sets of numerical tests show a good agreement between the predictions of the proposed viscoelastic workflow and numerical simulations for relatively high viscosities where viscoelastic effects are important.

The results confirm that application of extended Gassmann equations in conjunction with the complex and frequency-dependent moduli of viscoelastic pore filling material, such as heavy oil, provides a good approximation for the elastic moduli of rocks saturated with such material. By construction, this approximation is exactly consistent with the classical Gassmann's equation for sufficiently low frequencies or high temperature when heavy oil behaves like a fluid. For higher frequencies and/or lower temperatures, the predictions are in good agreement with the direct numerical solution of equations of dynamic viscoelasticity on the microscale. This demonstrates that the proposed methodology provides realistic estimates of elastic properties of heavy oil rocks.

Key words: Microstructure; Elasticity and anelasticity; Wave propagation; Acoustic properties; Mechanics, theory, and modeling.

INTRODUCTION

Heavy oils are emerging as a substantial hydrocarbon reserve, which is usually exploited using thermal recovery processes. As with conventional oil and gas, the seismic method can be used both for reservoir characterization and for production monitoring. To this end, rock physics relationships are required to link seismic parameters to the properties of oil as a function of frequency and thermodynamic (pressure, volume and temperature) conditions. In recent years, a number of laboratory measurements of elastic properties of heavy oils and of rocks saturated with heavy oil have been reported (Nur *et al.* 1984; Eastwood 1993; Schmitt 1999; Batzle *et al.* 2006). According to these measurements, heavy oils exhibit viscoelastic properties such that at low frequencies they behave like liquids, but at high frequencies almost like solids. At intermediate frequencies, the elastic moduli are complex, exhibiting strong attenuation and velocity dispersion. The characteristic frequency of this viscoelastic transition is strongly dependent on temperature, such that oil which at room temperature behaves as a nearly elastic solid (over a wide range of frequencies), can exhibit Newtonian fluid behaviour at temperatures above 200 °C. The overview of heavy oil reserves and the recent development in this direction can be found in Batzle *et al.* (2006), Hinkle & Batzle (2006) and Han *et al.* (2007a,b).

While the properties of bulk heavy oil can be approximated by an appropriate viscoelastic model, very few attempts to model the properties of rocks saturated with heavy oil have been reported (Eastwood 1993; Leurer & Dvorkin 2006; Gurevich *et al.* 2008). The rock physics for heavy oil is different from the rock physics for conventional fluids, because the viscoelastic rheology of heavy oil makes the Gassmann's and Biot's theories not applicable. Indeed, the Gassmann's theory assumes that the fluid pressure is equilibrated throughout all the pore space of the rock. If the medium is saturated with a Newtonian fluid, this is ensured by Pascal's law, which, in the absence of body forces, is valid in the static limit. The heavy oils, however, are viscoelastic and have non-zero shear moduli even at seismic frequencies; therefore Pascal's law does not apply. Similarly, Biot's theory (Biot 1962) assumes that the shear stresses in the fluid are negligible compared to the shear stresses in the solid matrix, an assumption which does not hold for viscoelastic media. Both Gassmann's and Biot's theories may still be valid at sufficiently low frequencies where heavy oil behaves like a Newtonian fluid; however, for very heavy oils and bitumen at typical subsurface temperatures this will only be at frequencies much lower than seismic frequencies.

Since properties of viscoelastic materials are frequency-dependent, it is natural to consider them in the frequency domain. For a given frequency, a viscoelastic solid is approximately equivalent to an elastic medium with complex bulk and shear moduli. In particular, in the quasi-static limit, effective properties of a mixture of viscoelastic materials (or viscoelastic with elastic materials) can be obtained by any mixing scheme developed for elastic materials, by substituting complex moduli of constituent viscoelastic media for the elastic moduli (Hashin 1970). For porous rocks saturated with an elastic material, a simple mixing scheme known as the extended Gassmann (EG) equations has recently been proposed by Ciz & Shapiro (2007). The EG mixing scheme has an inherent advantage that when the pore filling material is fluid, its results coincide with the classical Gassmann's equation, which is exact for fluid-saturated materials.

In this paper, we extend the EG scheme of Ciz & Shapiro (2007) to rocks saturated with a viscoelastic material, by substituting the complex (and frequency-dependent) moduli of the viscoelastic material for the moduli of the pore fill. We then test the predictions of this scheme against numerical simulations performed on the pore scale.

The paper is organized as follows. First, we briefly review the viscoelastic rheology of heavy oils, Gassmann's equation for fluid-saturated rocks and its extension to rocks saturated with an elastic material (EG equations of Ciz & Shapiro 2007). We then generalize the EG scheme to rocks saturated with a viscoelastic material. The final section of the paper is devoted to numerical validation of the scheme. Here, we perform viscoelastic numerical simulations of wave propagation of elastic waves in pore-scale mixtures of elastic and viscoelastic materials. The simulations of the wave propagation are performed using the viscoelastic extension of the displacement–stress rotated staggered finite-difference (VRSG FD) grid numerical technique developed by Saenger *et al.* (2005). The numerical results are compared with the predictions of the viscoelastic EG scheme.

THEORETICAL BACKGROUND

Gassmann fluid substitution

The Gassmann's equations (Gassmann 1951) predict effective elastic properties of an isotropic homogeneous bulk rock frame filled with a fluid. Gassmann's fluid substitution is commonly applied to predict the bulk modulus of rocks saturated with different fluids. This equation assumes that all pores are interconnected and the pore pressure is in equilibrium in the pore space. The porous frame is macroscopically and microscopically homogeneous and isotropic. Fluid-saturated bulk and shear moduli according to Gassmann (1951) yield

$$K_{\rm sat}^{-1} = K^{-1} - \frac{\left(K^{-1} - K_{\rm g}^{-1}\right)^2}{\phi\left(K_{\rm f}^{-1} - K_{\rm g}^{-1}\right) + \left(K^{-1} - K_{\rm g}^{-1}\right)}, \tag{1}$$

and

$$\mu_{\rm sat} = \mu, \tag{2}$$

where $K_{\rm sat}$ and $\mu_{\rm sat}$ are fluid-saturated bulk and shear moduli, K and μ are drained bulk and shear moduli, $K_{\rm g}$ is grain bulk modulus, $K_{\rm f}$ is bulk modulus of the pore fluid and ϕ is porosity.

Generalized Gassmann's equations for porous media saturated with an elastic solid material

Consider a porous rock with an uniformly distributed porosity, ϕ, whose pores are filled with an elastic solid material. The infill solid body is composed of the elastic material described by the elastic bulk and shear moduli $K_{\rm ifm}$ and $\mu_{\rm ifm}$, and a density $\rho_{\rm ifm}$. The drained solid frame formed from grains and pore spaces is characterized by bulk and shear moduli and density K, μ, ρ, respectively, and steady state permeability κ. The grains of the solid frame are characterized by bulk and shear moduli $K_{\rm g}, \mu_{\rm g}$ and density $\rho_{\rm g}$.

According to Ciz & Shapiro (2007), the generalized Gassmann's equations for the isotropic solid infill of the pore space and for the isotropic inhomogeneous material building up the rock frame yield the 'solid-saturated' bulk and shear moduli.

$$K_{\rm sat}^{-1} = K^{-1} - \frac{\left(K^{-1} - K_{\rm g}^{-1}\right)^2}{\phi\left(K_{\rm if}^{-1} - K_{\phi}^{-1}\right) + \left(K^{-1} - K_{\rm g}^{-1}\right)}, \tag{3}$$

and

$$\mu_{\rm sat}^{-1} = \mu^{-1} - \frac{\left(\mu^{-1} - \mu_{\rm g}^{-1}\right)^2}{\phi\left(\mu_{\rm if}^{-1} - \mu_{\phi}^{-1}\right) + \left(\mu^{-1} - \mu_{\rm g}^{-1}\right)}, \tag{4}$$

where $K_{\rm if}$ and $\mu_{\rm if}$ are effective bulk and shear moduli related to the average deformation of the pore filling solid material, K_ϕ and μ_ϕ are related to the average deformation of the rock frame pore volume.

For the homogeneous isotropic rock frame ($K_\phi = K_{\rm g}, \mu_\phi = \mu_{\rm g}$) eqs (3)–(4) reduce to

$$K_{\rm sat}^{-1} = K^{-1} - \frac{\left(K^{-1} - K_{\rm g}^{-1}\right)^2}{\phi\left(K_{\rm if}^{-1} - K_{\rm g}^{-1}\right) + \left(K^{-1} - K_{\rm g}^{-1}\right)} \tag{5}$$

and

$$\mu_{\rm sat}^{-1} = \mu^{-1} - \frac{\left(\mu^{-1} - \mu_{\rm g}^{-1}\right)^2}{\phi\left(\mu_{\rm if}^{-1} - \mu_{\rm g}^{-1}\right) + \left(\mu^{-1} - \mu_{\rm g}^{-1}\right)}. \tag{6}$$

The above expressions can be rewritten in the following form:

$$K_{\rm sat} = K + \alpha^2 M, \tag{7}$$

where

$$\frac{1}{M} = \frac{\phi}{K_{\rm if}} + \frac{\alpha - \phi}{K_{\rm g}}, \qquad \alpha = 1 - \frac{K}{K_{\rm g}} \tag{8}$$

and

$$\mu_{\rm sat} = \mu + \beta^2 N, \tag{9}$$

where

$$\frac{1}{N} = \frac{\phi}{\mu_{\rm if}} + \frac{\beta - \phi}{\mu_{\rm g}}, \qquad \beta = 1 - \frac{\mu}{\mu_{\rm g}}. \tag{10}$$

The eqs (7)–(10) represent the isotropic 'Gassmann's equations' for the 'solid-saturated' porous frame. Note that the equations for the 'solid-saturated' bulk and shear moduli are of the same form.

If the pore filling material is a fluid, eqs (7)–(10) reduce to Brown–Korringa (1975) equations. In the case of a single mineral in the skeleton frame and a fluid in the pore space, Brown–Korringa equations reduce to the classical Gassmann's eqs (1)–(12).

As shown by Ciz & Shapiro (2007), when the bulk and shear moduli $K_{\rm ifm}$ and $\mu_{\rm ifm}$ of the pore filling material are on the same order of magnitude as the respective grain moduli $K_{\rm g}$ and $\mu_{\rm g}$, the effective bulk and shear moduli $K_{\rm if}$ and $\mu_{\rm if}$ can be approximated by the moduli $K_{\rm ifm}$ and $\mu_{\rm ifm}$, respectively.

PROPOSED METHODOLOGY

Application of extended Gassmann equations to rocks saturated with a viscoelastic material

Generalized Gassmann eqs (5) and (6) can be extended to viscoelastic pore filling material using the elastic/viscoelastic correspondence principle (Hashin 1970). This can be done by simply replacing in eqs (5) and (6) the elastic moduli of solid infill with the frequency-dependent bulk and shear moduli $K_{\rm ifm}(\omega)$ and $\mu_{\rm ifm}(\omega)$ of the viscoelastic infill material. To do this, we need to know the rheology of the viscoelastic material, that is, the dependency of these moduli on frequency ω and temperature T. In this work, we assume the simplest Maxwellian rheology of the heavy oil, where the shear modulus is given by

$$\mu_{\rm ifm}(\omega) = \frac{\mu_\infty}{\frac{-i\mu_\infty}{\omega\eta} + 1} \tag{11}$$

and

$$K_{\rm ifm}(\omega) = K_f + \frac{5}{3}\frac{\mu_\infty}{\frac{-i\mu_\infty}{\omega\eta} + 1}, \tag{12}$$

where μ_∞ is the (real) shear modulus of the infill medium in the high-frequency limit, η is the dynamic shear viscosity of the same medium at low frequencies and $\rho = (1-\phi)\rho_{\rm g} + \phi\rho_{\rm f}$ is the overall density.

As mentioned earlier, behaviour of heavy oils is also strongly dependent on temperature. For a Maxwell body, this dependency can be expressed through the relationship between the low-frequency viscosity, η, and temperature. Following Beggs & Robinson (1975), we assume that the viscosity η in 'cPoise' of a gas-free oil is given by

$$\mathrm{Log}_{10}(\eta + 1) = 0.505y(17.8 + T)^{-1.163}, \tag{13}$$

with

$$\mathrm{Log}_{10}(y) = 5.693 - 2.863/\rho_0, \tag{14}$$

where T is temperature in °C and ρ_0 (kg m^{-3}) is reference density measured at 15.6 °C and at the atmospheric pressure. We set $\rho_0 = 1000$ kg m^{-3}.

We note that the Maxwell rheology of heavy oil as given by eqs (11) and (12) is chosen here for its simplicity and is not intended to represent the rheology of real heavy oils. Realistic rheology of heavy oils is a subject of intense research and is beyond the scope of this paper. The generalized Gassmann's equations for viscoelastic infill are not at all limited to this rheology and can be used in conjunction with any other rheology, such as Cole–Cole model (Batzle *et al.* 2006). Alternatively, the viscoelastic moduli $K_{\rm ifm}(\omega)$ and $\mu_{\rm ifm}(\omega)$ for given frequencies and temperatures can be substituted directly from rheometric measurements (Behura *et al.* 2007).

Summary of the modelling

We summarize the modelling approach in the following steps:

(1) First, we need to know elastic moduli K and μ of the dry rock frame. These moduli can be known from laboratory measurements or estimated from theoretical or empirical rock physics models. In numerical tests described below, we assume a particular geometry of the pore space. Therefore, we can simply compute the effective elastic moduli, K and μ, of the rock frame by assuming that the bulk and shear moduli of the pore filling material are zero.

(2) We define the viscoelastic model for the viscous infill. In this paper, we use the Maxwellian rheology model given by eqs (11) and (12).

(3) The complex moduli, $K_{\rm ifm}$ and $\mu_{\rm ifm}$, of the viscoelastic pore fill are substituted into the generalized Gassmann's eqs (5)–(6). These equations yield the effective elastic moduli, $K_{\rm sat}$ and $\mu_{\rm sat}$, for the rock saturated with a viscous infill material, such as heavy oil.

(4) *P*- and *S*-wave seismic velocities are obtained from the 'saturated' elastic moduli, $K_{\rm sat}$ and $\mu_{\rm sat}$, using standard eqs (B1) and (B2) from Appendix B.

In the following, we test the validity of this workflow by comparing its prediction with a direct numerical solution of dynamic equations of viscoelasticity on the microscale.

NUMERICAL VALIDATION

Approach

To test the validity of the proposed methodology for modelling elastic properties of porous rocks saturated with a viscoelastic pore fill, we perform a number of numerical simulations on the pore scale, and compare these results with the predictions of the EG equations. The simulations are performed for a reflection setup shown schematically in Fig. 1. The simulation setup consists of a free fluid on the left-hand side and a porous medium on the right-hand side; the two media are separated by a flat interface. The aim of the simulations is to compute the reflection response of the fluid/porous solid interface for an incident wave coming to the interface from the free fluid.

The simulations of the wave propagation are performed using the VRSG FD grid numerical technique developed by Saenger *et al.* 2005 (see Appendix A). This technique, which consists in solving numerically the equations of dynamic viscoelasticity on the microscale, allows us to compute reflection coefficients for a given rheology of the pore filling material. The viscoelastic behaviour of the pore filling material is described in the modelling algorithm as a generalized Maxwell body as described in the previous section. As illustrated in Fig. 2, for a given frequency the Maxwell body is equivalent to a Newtonian fluid at low viscosities and to an elastic solid in the limit of high viscosities.

The VRSG FD technique allows us to simulate and analyse both poroelastic and viscoelastic phenomena of wave propagation in heavy oil rocks. The reflection setup has been chosen for this work (in contrast to a more conventional transmission setup), because

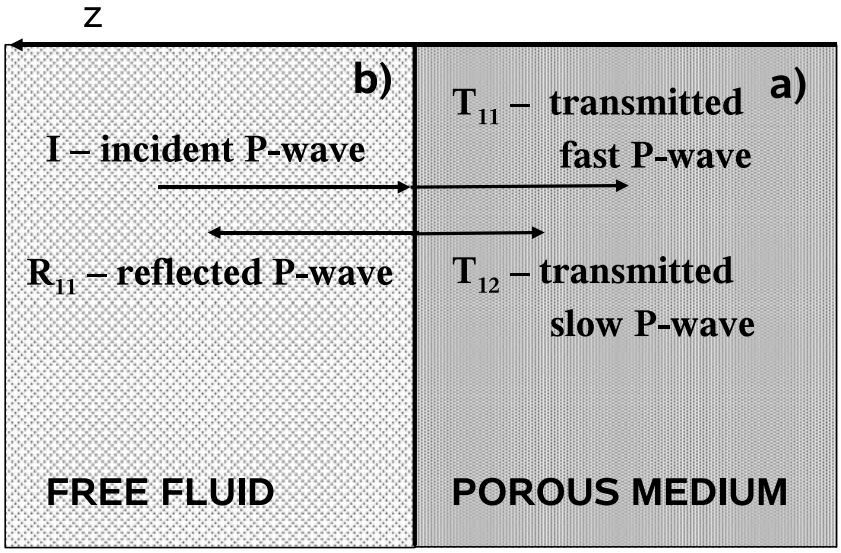

Figure 1. Reflection and transmission from an interface of a porous medium/fluid (a and b, respectively). In a poroelastic half-space, two *P* waves propagate—a fast compressional wave and the Biot's second bulk compressional mode.

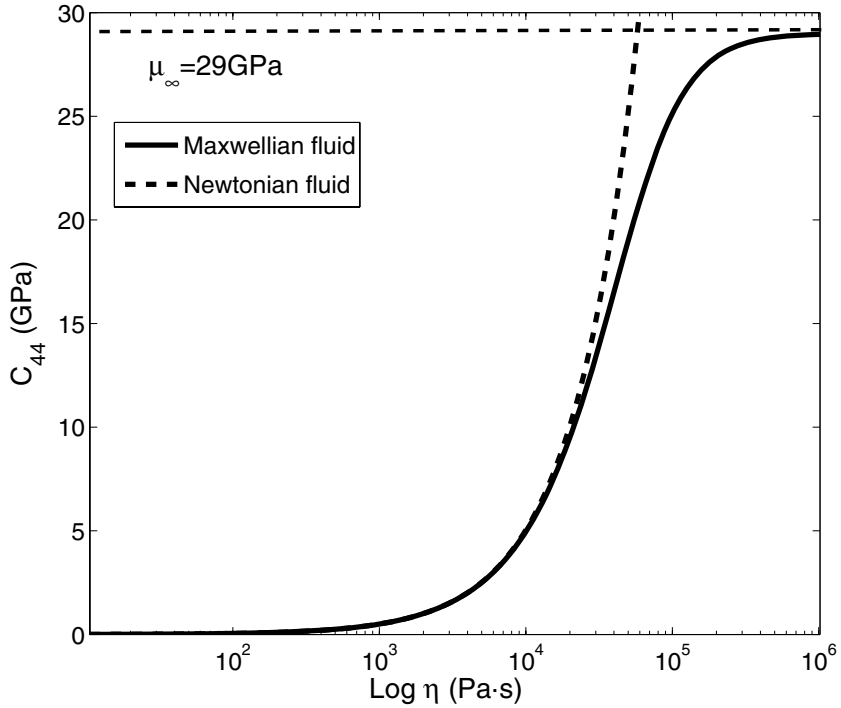

Figure 2. Newtonian and Maxwellian rheological models. In a wide range of fluid viscosities, the Newtonian fluid model is identical to the Maxwellian model. The deviation is seen for viscosities $\eta > 1000$ Pa s, thus in the viscosity range typical for heavy oil reservoirs.

reflection coefficients are more sensitive to the properties of the porous media and the pore fill. For instance, for the Newtonian pore fluids, the reflection coefficient between the free fluid and a porous medium is much more sensitive to the viscosity of the pore fluid than is the effective velocity of the transmitted waves (Denneman *et al.* 2002; Gurevich *et al.* 2004).

We perform numerical tests for an idealized 2-D porous medium consisting of alternating solid and viscoelastic layers, and for a more realistic 3-D porous medium. The details of the two sets of numerical tests are described below.

Results of 2-D modelling

First, we performed numerical simulations of reflections from an interface between a free fluid and a an idealized porous medium composed from alternating layers of an elastic solid and viscoelastic medium (Fig. 3). Such an idealized system has many features of a fluid-saturated porous medium (Bedford 1986). The advantage of such a simple geometry is that poroelastic parameters described by the Biot's theory of poroelasticity can be obtained. These parameters depend only on the elastic properties of the solid and fluid

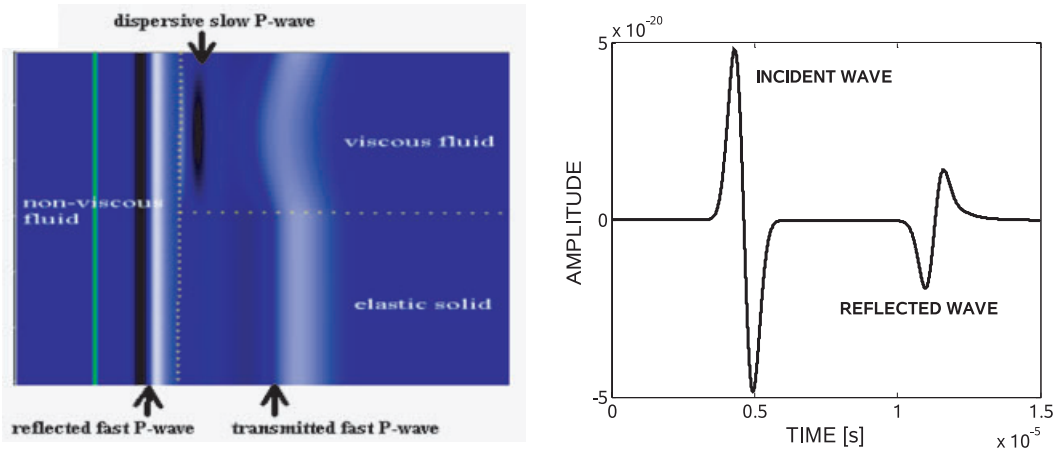

Figure 3. Reflection and transmission from an interface of the idealized porous medium composed of alternating elastic solid and viscous fluid layers and a free liquid. The snapshot of the displacement field is shown on the left-hand side. The transmitted fast compressional wave and the dispersive second bulk compressional mode can be identified in the idealized porous medium. The reflected compressional wave propagates in the free liquid. A seismogram recorded on the line of receivers in the free liquid shows an incident and a reflected *P* wave.

constituents and layer thickness. For computation of poroelastic reflection coefficient in expressions (C1) and (C2), a permeability, κ_a, is required. For our idealized 2-D porous medium, the permeability is $\kappa_a = \phi\, h_{\rm f}^2/12$, where porosity $\phi = h_{\rm f}/(h_{\rm f} + h_{\rm s})$, $h_{\rm f}$ and $h_{\rm s}$ are the thicknesses of fluid and solid layers (Bedford 1986). Drained elastic moduli, K_a and μ_a, are obtained using Backus average (Backus 1962).

We perform normal incidence reflection of the plane *P* wave from the idealized porous interface. The free fluid part of the model (60 × 1000 gridpoints) is water with *P*-wave velocity $v_{pb} = 1490\,{\rm m\,s^{-1}}$ and density $\rho_b = 1000\,{\rm kg\,m^{-3}}$. The porous medium consists of two horizontal thin layers—a viscoelastic layer (for low viscosities equivalent to a Newtonian fluid) and an elastic solid layer. Both layers are equal in size (30 × 2000 gridpoints). The periodic boundary conditions at top and bottom of the model ensure the periodicity of this layered system.

Our numerical model is built with spatial step $\Delta x = 0.00001$ m. The solid layer has *P*-wave velocity $v_P = 5100\,{\rm m\,s^{-1}}$, *S*-wave velocity $v_S = 2944\,{\rm m\,s^{-1}}$ and density $\rho_s = 2540\,{\rm kg\,m^{-3}}$. For the viscoelastic layer, we set elastic parameters $c_{11} = 3.922 \times 10^{11}$ Pa, $c_{44} = 1.3 \times 10^{11}$ Pa, and $\rho_f = 1000\,{\rm kg\,m^{-3}}$ (high-frequency limits of the numerical approach; the resulting *P*-wave velocity at 0 Hz is $v_P(0\,{\rm Hz}) = 1490\,{\rm m\,s^{-1}}$; see Saenger *et al.* 2005, for details). The viscosity is varied from 0.1 to 10^7 Pa s. To generate a *P* wave, we use a vertical line source with a Ricker wavelet of dominant frequency $f_{\rm dom} = 500$ kHz, and width $\Delta t = 5 \times 10^{-10}$ s. The *z*-displacement snapshot of the 2-D wavefield in Fig. 3 shows a reflected wave in the free fluid, a transmitted fast *P* wave in the porous medium (solid and viscoelastic layers) and a transmitted dispersive Biot's second compressional mode in viscoelastic layers. The reflection coefficient is estimated as a ratio of the incident and the reflected amplitude recorded at the position of the receiver line (in the middle of the left part of the model). All the computations are carried out with second-order spatial finite-difference operators and with a second-order time update.

The results of reflection from poroelastic interface of idealized medium are summarized in Fig. 4. This figure shows the variation of reflection coefficients, R_{11}, with the viscosity of the pore infill. The diamonds represent reflection coefficients obtained by numerical simulations. The thick solid line shows the equivalent elastic reflection coefficient (Appendix B) and the dashed line the reflection coefficient computed using the viscoelastic EG equations introduced in this paper. The thin solid line corresponds to the poroelastic solution given by eq. (C1). The dashed line shows a combined poroelastic solution extended to viscoelasticity as described below.

Whereas the elastic reflection coefficient from a single interface is independent of viscosity, the numerical results show substantial variation with viscosity. There are two reasons for these variations. At high viscosities, this variation is due to viscoelastic effects, and is well described by the viscoelastic Gassmann's equations introduced in this paper. At lower viscosities, where the pore filling material is essentially equivalent to a Newtonian fluid (see Fig. 2), the deviation from the elastic reflection coefficient is due to the wave-induced flow of the pore fluid across the interface. This effect is not accounted for in EG equations. However, as can be seen in Fig. 4, it is well described by a theoretical solution based on the Biot's theory of poroelasticity (see Appendix C). This poroelastic solution has been developed for a porous medium saturated with a Newtonian fluid. It can be extended to viscoelastic pore filling material by combining it with the viscoelastic EG equations. The resulting solution is shown in Fig. 4 as a dashed line and shows a good agreement with the numerical solution in a broad range of viscosities.

The discrepancy of the numerical results from the poroelastic solution at low viscosities is caused by the violation of the low-frequency assumption required for the analytical solution derived by Gurevich *et al.* (2004) and by the insufficient sampling of the viscous skin depth discussed by Ciz *et al.* (2006) and Saenger *et al.* (2007). The dominant frequency $f_{\rm dom} = 500$ kHz of the propagating wavelet is not in the low-frequency range of Biot's theory of poroelasticity for viscosities lower than 1 Pa s. Furthermore, for viscosities lower than 0.1 Pa s, the sampling of the viscous skin depth may be inadequate.

Results of 3-D modelling

Next, we perform numerical simulations of elastic wave propagation in realistic synthetic 3-D digital rock models. These models were analysed in detail by Saenger *et al.* (2004, 2005). The model chosen

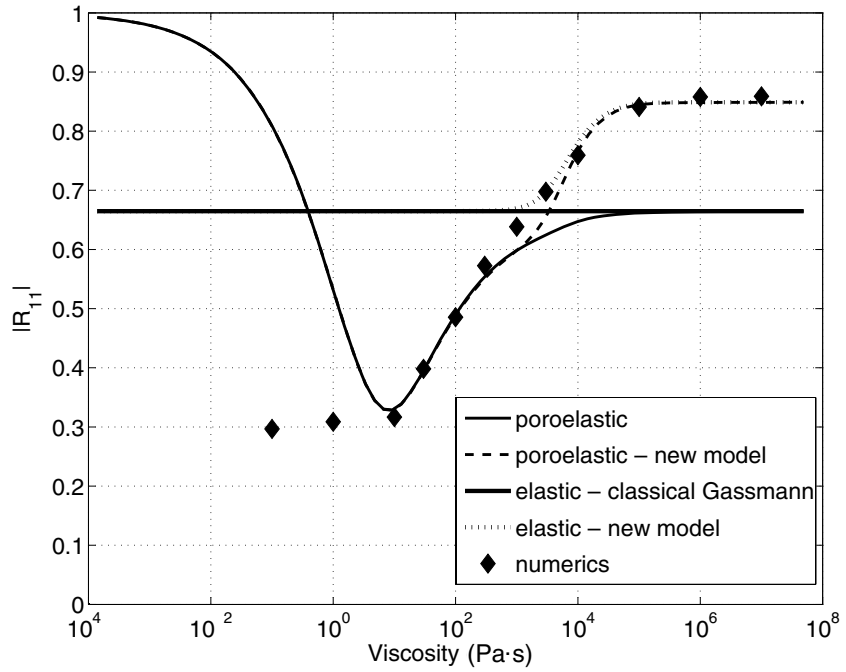

Figure 4. Reflection coefficient of a compressional P wave (R_{11}) recorded in a free liquid of the 2-D model and reflected from an idealized poroelastic medium. The discrete points (diamonds) represent values of reflection coefficients obtained from numerical simulations. Elastic and poroelastic solutions correspond to equations B4 and C1, respectively, whereas the new model computes seismic velocities using the generalized Gassmann's equations.

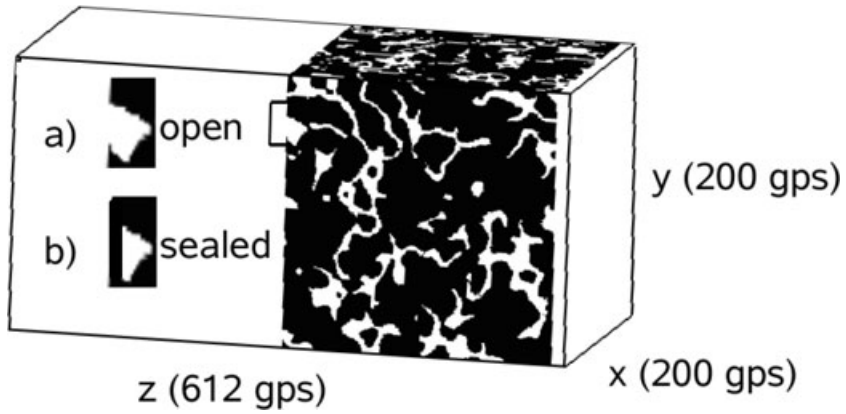

Figure 5. Scheme of the 3-D model for the interface between free fluid and 3-D porous structure (subsample of the GRF5) for an open (a) and a sealed (b) interface. The model size is 200 × 200 × 612 gridpoints (gps).

for our tests is shown schematically in Fig. 5. Our simulations are performed using a subsample of the Gaussian Random Field model 5 (GRF5). The drained bulk and shear moduli for GRF5 are $K_a = 0.344 \cdot K_g$, $\mu_a = 0.272\mu_g$ and the permeability, $\kappa_a = 647.6 \times 10^{-4} (\Delta x)^2$, where Δx represents the spatial step (Saenger *et al.* 2005). In our numerical setup, we use the spatial step $\Delta x = 0.0002$ m. The synthetic porous model is embedded in a homogeneous fluid or solid medium. The full model consists of 612 × 200 × 200 gridpoints. We perform our modelling experiments with periodic boundary conditions in the x- and y-directions. We apply a plane source on the left-hand side ($z = 0$ m) of the model. The plane P wave generated in this way propagates from the left-hand side of the model to the interface of a fluid (or solid) and a porous medium. We record the reflected wave in the fluid (solid). The source wavelet is the first derivative of the Gaussian with the dominant frequency $f_{\rm dom} = 80$ kHz and with the time increment of $\Delta t = 2.1 \times 10^{-8}$ s.

We perform two sets of reflection experiments: (1) the reflection between a free fluid and a porous medium saturated with a viscoelastic medium (for low viscosities equivalent to a Newtonian fluid) and (2) the reflection between an elastic solid and a porous medium saturated with a viscoelastic medium. In the first case, we perform the reflection for open and sealed interfaces (see Fig. 5). To numerically simulate the poroelastic effect at the open interface, we set bulk modulus of the free non-viscous fluid to the bulk modulus of water $K_{fb} = 2.22 \times 10^9$ Pa with a density of $\rho_{fb} = 1000$ kg m^{-3}. The solid has P-wave velocity, $v_P = 5100$ m s^{-1}, S-wave velocity, $v_S = 2944$ m s^{-1}, and density, $\rho_s = 2540$ kg m^{-3}. For the viscoelastic medium, the elastic parameters are $c_{11} = 90.000222 \times 10^9$ Pa, $c_{44} = 30 \times 10^9$ Pa and density $\rho_f = 1000$ kg m^{-3} (high-frequency

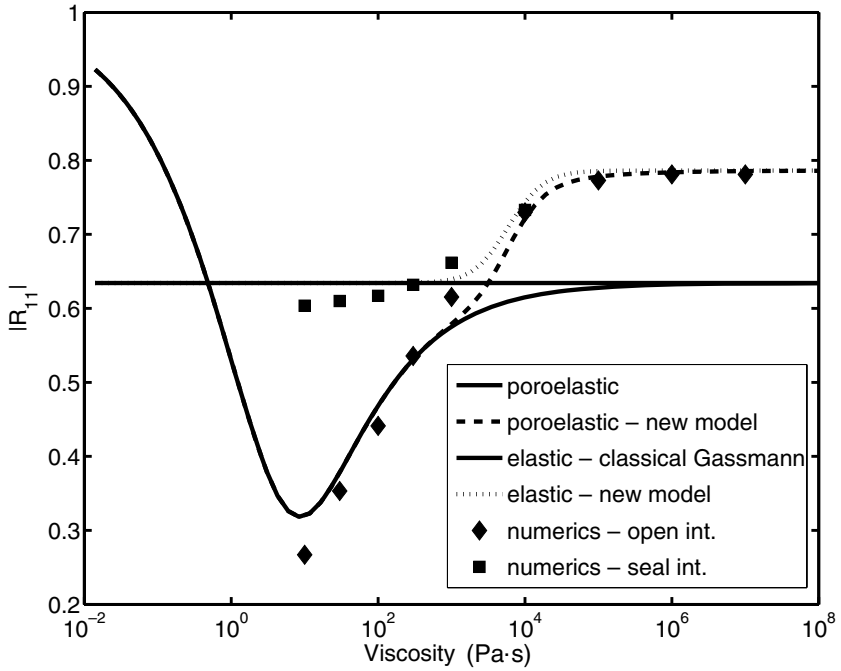

Figure 6. Reflection coefficient of a compressional *P* wave recorded in the free liquid in the 3-D model (subsample of the GRF5): free liquid/poroelastic medium. The discrete points (diamonds) represent values of reflection coefficients obtained from numerical simulations for an open interface whereas squares represent equivalent situation for a sealed interface. Poroelastic and elastic solutions correspond to eqs (B4) and (C1) whereas the new model computes seismic velocities using the generalized Gassmann's equations (3, 4, 11 and 12).

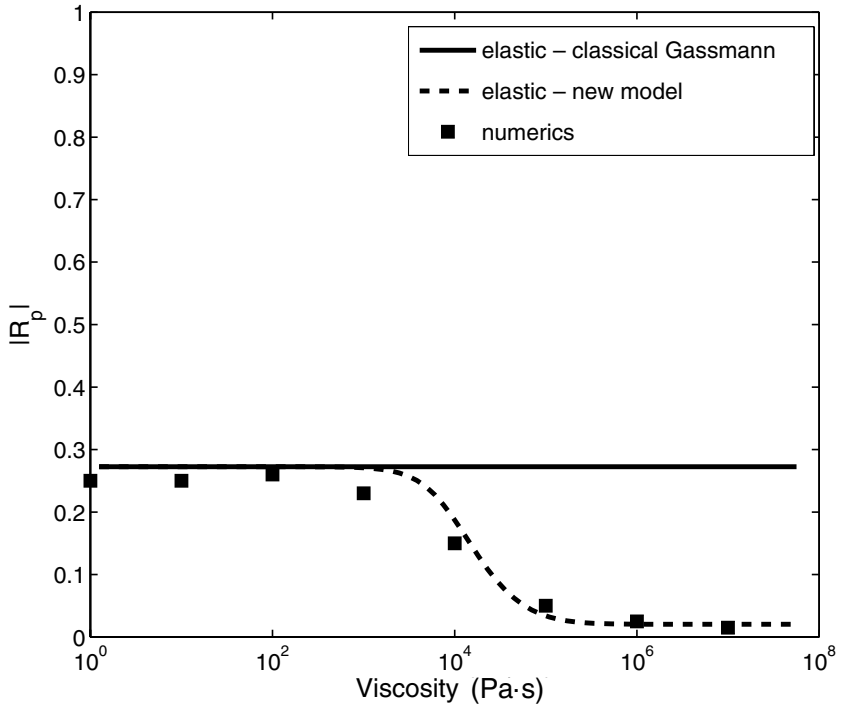

Figure 7. Reflection coefficients of the compressional waves recorded in an elastic solid in the 3-D model (subsample of the GRF5): elastic solid/poroelastic medium interface. The squares represent numerical simulations, the elastic model computes reflection coefficients using classical Gassmann's fluid substitution whereas the new model implements generalized Gassmann's equations for the solid infill of the pore space.

limits of the numerical approach; the resulting bulk modulus at 0 Hz is $K_{fa} = 0.222 \times 10^6$ Pa; see Saenger *et al.* 2005, for details). Such unrealistically low bulk modulus of the pore fill is chosen to magnify the poroelastic effect on reflection coefficient, and hence to provide an additional consistency test for numerical simulations. The fluid viscosity is varied from 10 to 10^7 Pa s.

The results are shown in Fig. 6. Numerically calculated reflection coefficients are in very good agreement with poroelastic reflection

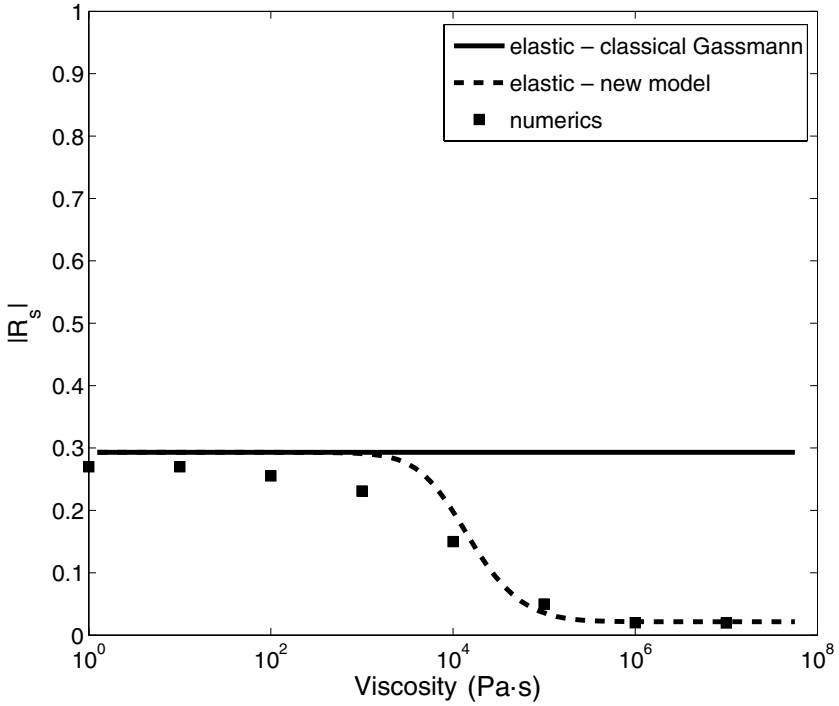

Figure 8. Reflection coefficients of the shear waves recorded in an elastic solid in the 3-D model (subsample of the GRF5): elastic solid/poroelastic medium interface. This is the same situation as in Fig. 7 for compressional waves.

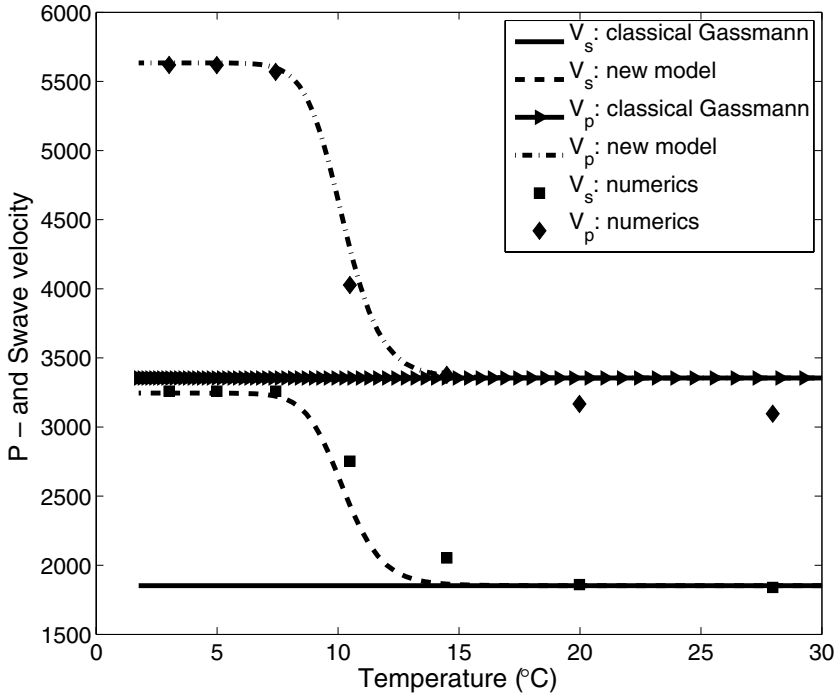

Figure 9. *P*- and *S*-wave velocities in dependence of the temperature. The classical Gassmann's model for seismic velocities is compared with the generalized Gassmann's equations and numerical simulations.

coefficients given by eq. (C1) at low viscosities. We show here the poroelastic effect which occurs at the open interface of the free fluid and the fluid-saturated porous medium. The energy of the incident wave from the free fluid is in the porous medium redistributed into the fast *P* wave and second compressional mode (see Figs 1 and 6). According to Gurevich *et al.* (2004), the fluid flow is significant when the contrast between bulk moduli of free fluid and pore fluid is large (as used in our numerical example). In the case of a sealed interface, the numerical simulations correspond to an equivalent elastic reflection given by classical Gassmann's model in eq. (B4). At high viscosities, numerically simulated data deviate from the analytical models (C1) and (B4). Implementation of the generalized

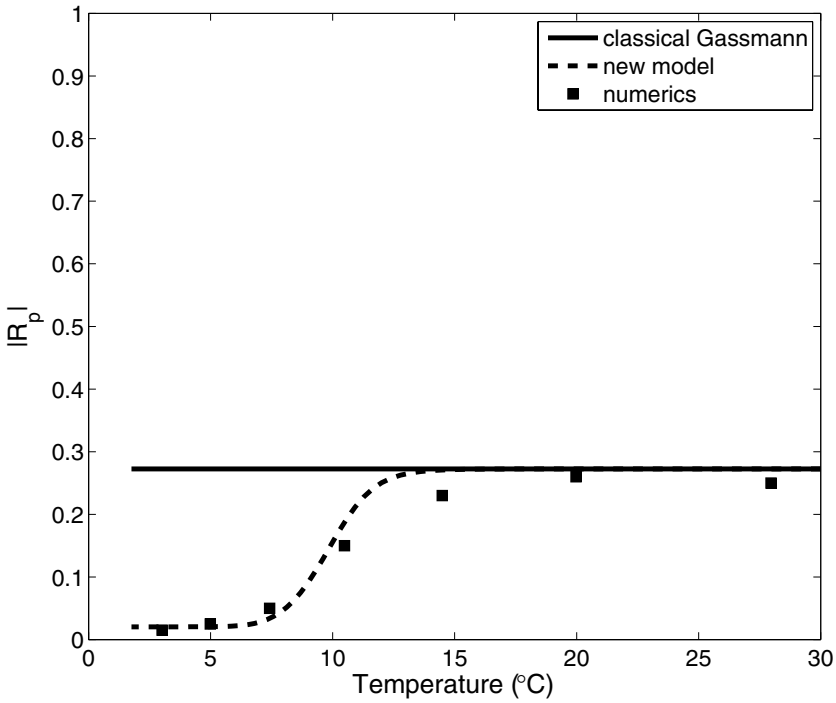

Figure 10. *P*-wave reflection coefficients as a function of temperature. The equivalent elastic reflection coefficient is compared with both reflection coefficients implementing the generalized Gassmann's equations for the solid infill of the pore space and numerical simulations.

Gassmann's eqs (5)–(6) describes well the output obtained from the numerical simulations in the 3-D realistic digital rock models.

The results for the reflection between an elastic solid and a saturated porous medium are shown in Figs 7 and 8. The parameters of the model are the same as in the case (1) except for the bulk modulus of the viscous pore fluid being $c_{11} = 89 \times 10^9$ Pa, $c_{44} = 29 \times 10^9$ Pa and $\rho_f = 1000$ kg m^{-3} (high-frequency limits of the numerical approach; the resulting bulk modulus at 0 Hz is $K_{fa} = 2.22 \times 10^9$ Pa; see Saenger *et al.* 2005, for details). We observe that numerical results correlate well with the equivalent elastic solution which incorporates our generalized Gassmann's equations for the solid infill of the pore space. This situation is similar to the previous case with sealed interface where no fluid flow occurs over the interface. The decrease in the reflection coefficients at high viscosities is the result of the viscoelastic stiffening of the porous rock at high viscosities.

To study the temperature dependence of the reflection coefficients the relationship (13) is implemented into eqs (C1)–(B4) through the viscoelastic fluid models (11) and (12). The results are shown in Fig. 9. In this figure, we plot *P*- and *S*-wave effective velocities as a function of temperature. In Fig. 10, we show the same dependency for the reflection coefficients of the *P* wave. At low temperatures, we observe the deviation from the equivalent elastic model for *P*- and *S*-wave velocities given by eqs (B1) and (B2). The viscosity of the pore filling fluid (heavy oil) increases at low temperatures and consequently the overall stiffness of the porous structure increases.

CONCLUSIONS

We have developed a new model for elastic properties of rocks saturated with heavy oil. The heavy oil itself is represented by a viscoelastic material, which at low frequencies and/or high temperatures behaves as a Newtonian fluid, and at high frequencies and/or low temperatures as a nearly elastic solid. The bulk and shear moduli of a porous rock saturated with such viscoelastic material are then computed using approximate EG equations of Ciz and Shapiro by replacing the elastic moduli of the pore filling material with complex and frequency-dependent moduli of the viscoelastic pore fill.

We have tested the proposed methodology by comparing its predictions with numerical simulations based on a direct finite-difference solution of equations of dynamic viscoelasticity. The simulations were performed for the reflection coefficient from an interface between a homogeneous fluid and a porous medium. The first set of numerical tests was performed for an idealized porous medium consisting of alternating solid and viscoelastic layers. The second set was performed for a more realistic 3-D geometry of the pore space. Both sets of numerical tests show a good agreement between the predictions of the proposed viscoelastic workflow and numerical simulations for high viscosities. For lower viscosities, where the pore filling material essentially behaves as a Newtonian fluid, and where viscoelastic effects are negligible, the numerical results show systematic deviation from the viscoelastic solution. This deviation is caused by the wave-induced fluid flow across the fluid/porous solid interface, and is well described by an analytical solution based on Biot's equations of poroelasticity. The deviation is only observed when the pores are open at the interface, so that the pore fill comes into direct contact with the free fluid on the other side of the interface. As expected, this effect disappears when the interface is sealed, and also when the fluid is replaced by a homogeneous elastic solid.

Our results confirm that application of EG equations in conjunction with the complex and frequency-dependent moduli of viscoelastic pore filling material, such as heavy oil, provides a good approximation for the elastic moduli of rocks saturated with such material. By construction, this approximation is exactly consistent with the classical Gassmann's equation for sufficiently low

frequencies or high temperature when heavy oil behaves like a fluid. For higher frequencies and/or lower temperatures, the predictions are in good agreement with the direct numerical solution of equations of dynamic viscoelasticity on the microscale. This demonstrates that the proposed methodology provides realistic estimates of elastic properties of heavy oil rocks.

ACKNOWLEDGMENTS

The work was supported by the PHASE consortium at the Freie Universität Berlin. E.H. Saenger thanks the DFG (Deutsche Forschungsgemeinschaft) for the financial support through the Heisenberg Programm (SA 996/1-1). The authors are grateful to Bruce M. Hartley and Dina Makarynska for helpful comments.

REFERENCES

Backus, G., 1962. Long-wave elastic anisotropy produced by horizontal layering, *J. geophys. Res.,* **67,** 4427–4440.

Batzle, M., Hofman, R. & Han, D.-H., 2006. Heavy oils—seismic properties, *Leading Edge,* **25**(6), 750–756.

Bedford, A., 1986. Application of Biot's equations to a medium of alternating fluid and solid layers, *J. Wave-Mater. Interac.,* **1,** 34–53.

Beggs, H.D. & Robinson, J.R., 1975. Estimating the viscosity of crude oil systems, *J. Petrol. Technol.,* **27,** 1140–1141.

Behura, J., Batzle, M., Hofmann, R. & Dorgan, J., 2007. Heavy oils: their shear story, *Geophysics,* **72,** E175–E183.

Biot, M.A., 1962. Mechanics of deformation and acoustic propagation in porous media, *J. Appl. Phys.,* **33,** 1482–1498.

Brekhovskikh, L. & Godin, O., 1990. *Acoustics of Layered Media,*Vol. 1, Springer-Verlag, Berlin.

Brown, R.J.S. & Korringa, J., 1975. On the dependence of the elastic properties of a porous rocks on the compressibility of the pore fluid, *Geophysics,* **40,** 608–616.

Ciz, R. & Shapiro, S.A., 2007. Generalization of Gassmann's equations for porous media saturated with a solid material, *Geophysics,***72,** A75–A79.

Ciz, R., Saenger, E.H. & Gurevich, B., 2006. Pore scale numerical modeling of elastic wave dispersion and attenuation in periodic systems of alternating solid and viscous fluid layers, *J. acoust. Soc. Am.,* **120**(2), 642–648.

Denneman, A.I.M., Drijkoningen, G.G., Smeulders, D.M.J. & Wapenaar, K., 2002. Reflection and transmission of waves at a fluid/porous-medium interface, *Geophysics,* **67,** 282–291.

Eastwood, J., 1993. Temperature-dependent propagation of P-waves and S-waves in Cold Lake oil sands: comparison of theory and experiment, *Geophysics,* **58,** 863–872.

Emmerich, H. & Korn, M., 1987. Incorporation of attenuation into time-domain computations of seismic wave fields, *Geophysics,* **52,** 1252–1264.

Gassmann, F., 1951. Über die Elastizität poröser Medien, *Vier. der Natur Gesellschaft,* **96,** 1–23.

Gurevich, B., Ciz, R. & Dennemann, A.I.M., 2004. Simple expressions for normal incidence reflection coefficients from an interface between fluid-saturated porous materials, *Geophysics,* **69,** 1372–1377.

Gurevich, B., Osypov, K., Ciz, R. & Makarynska, D., 2008. Modeling elastic wave velocities and attenuation in rocks saturated with heavy oil, *Geophysics,* **73,** E115–E122.

Han, D.-H., Yao, Q. & Zhao, H.-Z., 2007a. Complex properties of heavy oil sand, in *Proceedings of SEG/San Antonio 2007 Annual Meeting,* Expanded abstract, 1609–1613.

Han, D.-H., Zhao, H.-Z., Yao, Q. & Batzle, M., 2007b. Velocity of heavy oils, in *Proceedings of SEG/San Antonio 2007 Annual Meeting,* Expanded abstract, 1619–1623.

Hashin, Z., 1970. Complex moduli of viscoelastic composites. I. General theory and application to particulate composites, *Int. J. Solids Struc.,* **6,** 539–552.

Hinkle, A. & Batzle, M., 2006. Heavy oils: a worldwide overview, *Leading Edge,* **25,** 742–749.

Leurer, K.C. & Dvorkin, J., 2006. Viscoelasticity of precompacted unconsolidated sand with viscous cement, *Geophysics,* **71,** T31–T40.

Nur, A., Tosaya, C. & Thanh, D.V., 1984. Seismic monitoring of thermal enhanced oil recovery processes, in *Proceedings of SEG 1984 Annual International Meeting,* Expanded Abstracts, 337–340.

Saenger, E.H., Gold, N. & Shapiro, S.A., 2000. Modeling the propagation of elastic waves using a modified finite-difference grid, *Wave Motion,* **31**(1), 77–92.

Saenger, E.H., Krüger, O.S. & Shapiro, S.A., 2004. Numerical considerations of fluid effects on wave propagation: influence of the tortuosity, *Geophys. Res. Lett.,* **31,** L21613.

Saenger, E.H., Shapiro, S.A. & Keehm, Y., 2005. Seismic effects of viscous Biot coupling: finite difference simulations on micro–scale, *Geophys. Res. Lett.,* **32,** L14310.

Saenger, E.H., Ciz, R., Krüger, O.S., Schmalholz, S.M., Gurevich, B. & Shapiro, S.A., 2007. Finite-difference modeling of wave propagation on microscale: a snapshot of the work in progress, *Geophysics,* **72,** SM293–SM300.

Schmitt, D.R., 1999. Seismic attributes for monitoring of a shallow heated heavy oil reservoir: a case study, *Geophysics,* **64,** 368–377.

APPENDIX A: VISCOELASTIC EXTENSION OF ROTATED STAGGERED GRID — VRSG

In our numerical simulations, we use the finite-difference numerical code of Saenger *et al.* (2005). To model wave propagation in a solid–fluid mixture, we apply the displacement–stress rotated staggered finite-difference grid for the solution of the elastodynamic wave equation with a viscoelastic extension. The theoretical model of viscoelasticity is based on an approach described by Emmerich & Korn (1987) which incorporates viscosity of a pore saturating fluid in the form of generalized Maxwell body (GMB). The modified Hooke's law yields (Saenger *et al.* 2005)

$$\sigma_{ij} = c_{ijkl} e_{kl} + \sum_{m=1}^{n} \zeta_m^{ij}. \tag{A1}$$

In this equation, σ_{ij} denotes the stresses, c_{ijkl} is the elastic tensor and e_{kl} is the strain tensor. The number of relaxation mechanisms is equal to m. The anelastic functions ζ_m^{ij} are determined by

$$\zeta_m^{ij} + \omega_m \zeta_m^{ij} = \omega_m Y_m^{ijkl} e_{kl}, \tag{A2}$$

with Y_m^{ijkl} as the tensors of anelastic coefficients and ω_m as angular relaxation frequencies. The GMB frequency-dependent viscoelastic modulus $C_{ijkl}(\omega)$ can be derived by inserting the Fourier transform of eq. (A1) into eq. (A2):

$$C_{ijkl}(\omega) = c_{ijkl}(\omega) + \sum_{m=1}^{n} Y_m^{ijkl} \frac{\omega_m}{i\omega + \omega_m}. \tag{A3}$$

A compressible viscous fluid can be characterized by the following frequency-dependent elastic moduli (Newtonian fluid model):

$$C_{44}(\omega) = \mu(\omega) = i\omega\eta, \tag{A4}$$

$$C_{12}(\omega) = \lambda(\omega) = \lambda(0) + i\omega\eta \tag{A5}$$

with $\lambda(\omega)$ and $\mu(\omega)$ as angular-frequency-dependent Lamé parameters. For all examples in this paper, we assume that the viscosity of the fluid, η, is equal for both elastic constants. The comparison

of the Newtonian and Maxwellian rheological models is shown in Fig. 2. The detailed description of this algorithm can be found in Saenger *et al.* (2000, 2005).

APPENDIX B: EQUIVALENT ELASTIC MEDIUM—TRANSMISSION AND REFLECTION

The equivalent elastic medium represents the case of a jacketed (sealed interface) fluid-saturated poroelastic medium. The effective *P*- and *S*-wave velocities in such a medium are given by the classical Gassmann's (1951) eqs:

$$v_P = \sqrt{\frac{H}{\rho}} \tag{B1}$$

and

$$v_S = \sqrt{\frac{\mu}{\rho}}, \tag{B2}$$

where v_P and v_S are *P*- and *S*-wave velocities of the equivalent elastic medium. The parameter ρ represents the overall density $\rho = (1-\phi)\rho_{\rm g} + \phi\rho_{\rm f}$ with $\rho_{\rm g}$ and $\rho_{\rm f}$ being grain and fluid densities. The elastic modulus H is given by

$$H = L + \alpha C, \quad L = K + \frac{4}{3}\mu,$$
$$C = \alpha M, \quad M^{-1} = \frac{\alpha - \phi}{K_{\rm g}} + \frac{\phi}{K_{\rm f}}, \quad \alpha = 1 - \frac{K}{K_{\rm g}}, \tag{B3}$$

where α is the Biot's effective stress coefficient.

The reflection coefficient at normal incidence from the equivalent elastic medium yields the same equation as the familiar equation for an elastic medium (e.g. Brekhovskikh & Godin 1990):

$$R_{11} = \frac{\rho_b v_{1b} - \rho_a v_{1a}}{\rho_b v_{1b} + \rho_a v_{1a}}, \tag{B4}$$

where $\rho_{a(b)}$ and $v_{1a(b)}$ are the density and *P*- or *S*-wave velocities in the elastic media a and b. The parameter $\rho_{a(b)}$ represents overall density, $\rho_{a(b)} = (1-\phi)\rho_{ga(b)} + \phi\ \rho_{fa(b)}$. The *P*- and *S*-wave velocities, $v_{1a(b)}$, are given by the classical Gassmann's eqs (B1)–(B2). The reflection coefficient in the eq. (B4) is frequency independent.

APPENDIX C: REFLECTION FROM POROELASTIC INTERFACE

We assume an interface between a free fluid and a fluid-saturated poroelastic medium. If the half-space, b is a free fluid with density, ρ_b, and bulk modulus, K_b, one can derive the expressions for the reflection and transmission coefficients from an interface between a free fluid and a porous medium. This situation is shown in Fig. 1. An incident compressional wave in the free fluid (b) transforms into the reflected compressional wave in the fluid and two compressional waves in the poroelastic medium (a)—a fast *P*-wave and a second bulk compressional mode. Following Gurevich *et al.* (2004), the closed-form expression for the reflection coefficient reads

$$R_{11} = \frac{\rho_b v_{1b} - (1-Y)\rho_a v_{1a}}{\rho_b v_{1b} + (1+Y)\rho_a v_{1a}}, \tag{C1}$$

where the parameter Y is

$$Y = \left(\frac{C_a}{H_a} - 1\right)^2 \sqrt{\frac{i\omega\kappa_a}{\eta_a N_a}}\rho_b v_{1b}, \tag{C2}$$

and v_{1a} represents the *P*-wave velocity in the poroelastic half-space, v_{1b} denotes the *P*-wave velocity in the free fluid and ω is a frequency of the incident wave. Poroelastic parameters C_a, H_a and N_a are related as follows:

$$N_a = \frac{M_a L_a}{H_a}, \quad H_a = L_a + \alpha C_a, \quad L_a = K_a + \frac{4}{3}\mu_a,$$
$$C_a = \alpha M_a, \quad M_a^{-1} = \frac{\alpha - \phi}{K_{ga}} + \frac{\phi}{K_{fa}}, \quad \alpha = 1 - \frac{K_a}{K_{ga}}. \tag{C3}$$

The detailed analysis of the eq. (C1) was performed by Gurevich *et al.* (2004).